HAL
open science

Fatigue crack growth in thin notched woven glass composites under tensile loading. Part II: modelling

Matthieu Bizeul, Christophe Bouvet, Jean-Jacques Barrau, Rémy Cuenca

To cite this version:

Matthieu Bizeul, Christophe Bouvet, Jean-Jacques Barrau, Rémy Cuenca. Fatigue crack growth in thin notched woven glass composites under tensile loading. Part II: modelling. Composites Science and Technology, 2011, 71 (3), pp.297-305. 10.1016/j.compscitech.2010.11.017 . hal-01852319

HAL Id: hal-01852319

https://hal.science/hal-01852319

Submitted on 1 Aug 2018

HAL is a multi-disciplinary open access archive for the deposit and dissemination of scientific research documents, whether they are published or not. The documents may come from teaching and research institutions in France or abroad, or from public or private research centers.

L'archive ouverte pluridisciplinaire **HAL**, est destinée au dépôt et à la diffusion de documents scientifiques de niveau recherche, publiés ou non, émanant des établissements d'enseignement et de recherche français ou étrangers, des laboratoires publics ou privés.

Open Archive Toulouse Archive Ouverte (OATAO)
OATAO is an open access repository that collects the work of Toulouse researchers and makes it freely available over the web where possible.

This is an author -deposited version published in: http://oatao.univ-toulouse.fr/
Eprints ID: 4616

To link to this article: DOI:10.1016/j.compscitech.2010.11.017

URL: http://dx.doi.org/10.1016/j.compscitech.2010.11.017

To cite this version: BIZEUL Matthieu, BOUVET Christophe, BARRAU Jean-Jacques, CUENCA Rémy. Fatigue crack growth in thin notched woven glass composites under tensile loading. Part II: modelling. *Composites Science and Technology*, 2011, vol. 71, n° 3, pp. 297-305.
ISSN 0266-3538

Any correspondence concerning this service should be sent to the repository administrator: staff-oatao@inp-toulouse.fr

Fatigue crack growth in thin notched woven glass composites under tensile loading. Part II: Modelling

M. Bizeul [a], C. Bouvet [a,*], J.J. Barrau [a], R. Cuenca [b]

[a] Université de Toulouse, INSA, UPS, Mines Albi, ISAE, Institut Clément Ader, 10 av. E. Belin F-31077 Toulouse, France
[b] Eurocopter, 13725 Marignane, France

Keywords:
C. Finite element analysis (FEA)
A. Glass fibres
B. Fatigue
D. Life prediction

A B S T R A C T

Fatigue propagation of a through-the-thickness crack in thin woven glass laminates is difficult to model when using homogeneous material assumption. Crack growth depends on both the fatigue behaviour of the fibres and of the matrix, these two phenomena occurring at different time and space scales. The developed finite element model is based on the architecture of the fabric and on the fatigue behaviours of the matrix and the fibre, even if the pure resin and fibre behaviours are not used. That thus limits the physical meaning of this model. Basically, the objective of this simulation is to illustrate and to confirm proposed crack growth mechanism. The fatigue damage matrix is introduced with user spring elements that link the two fibre directions of the fabric. Fibre fatigue behaviour is based on the S–N curves. Numerical results are compared to experimental crack growth rates and observed damage in the crack tip. Relatively good agreement between predictions and experiments was found.

1. Introduction

Sandwich structures are often made of thin skins. Especially in laminates made of glass woven plies, a through-the-thickness crack could appear. The prediction of crack growth rate for primary structures loaded in fatigue has become very important.

A natural way for modelling the crack growth in composites is based on LEFM [1]. The main limitation of such developments is that the crack tip area with severe non-linear damage has to be small in comparison to the crack length. Further developments have led to the use of *J*-integral in order to take into account the damage zone in front of the crack tip. Shindo et al. [2] investigated the fatigue crack growth rate properties for GFRP laminates and have used such a concept due to the non-negligible size scale of damage occurred in crack tip.

An other way to take into account the damage zone that occurs in crack tip is to use the well-known Point Stress Criterion. Poe and Reeder [3] modelled the static failure of CNT and CT specimens in calculating critical tension and shear strains at characteristic distances. The influence of this progressive damage zone can also be judged with the help of cohesive crack model [4].

In order to have a better understanding of the notch tip phenomena, several authors [5,6] have tried to model the behaviour of the composite material through a continuum damage approach (CDM). Non-local criterion has been developed to improve the accuracy of the failure prediction in the case of large stress gradients.

Considering the experimental results of fatigue crack growth in woven glass laminates [7], the damage in woven plies is suggested to be considered in a localized manner. The LEFM concept fails to predict the crack growth rates for different specimen geometries [8]. First the proposed model is detailed, then the identification of parameters is carried out. The predicted results are finally compared with experimental data for each elementary lay-up sequence.

2. Modelling approach

The crack growth mechanism is a very complex process which starts with various matrix damage processes, like transverse cracking, longitudinal cracking, fibre debonding or delamination, that finally induces fibres failure and subsequently the crack growth. The objective of this simulation is to illustrate and to confirm a proposed crack growth mechanism, and in particular crack initiation effect on its growth. In order to achieve that, the idea is to try to separate the matrix damage effect with the fibre failure process. Nevertheless, in order to be coherent with an industrial application, only a partial separation of these two phenomena is taken into account. Indeed, the experimental tests used to calibrate the model are not pure experimental results on resin or fibres but always on woven fabrics. Therefore, the proposed model should be considered as a qualitative numerical illustration of a proposed crack growth mechanism.

* Corresponding author.
E-mail address: christophe.bouvet@isae.fr (C. Bouvet).

Under static tensile loading in the fibres direction, the stress–strain relationship of the chosen glass woven ply exhibits a change of slope usually called "knee-point" [9]. Pre- and post-knee behaviours are quite linear. This phenomenon is commonly associated with microcracks in the transverse fibre yarns which subsequently reach the warp and weft interface in the undulation areas within the same layer [10]. These typical damages in woven plies also occur under fatigue tensile loads [11]. So, the degradation in woven plies loaded in tension along the fibre direction in static and even in fatigue, not only tends to damage the matrix in the yarns but also unlinks the warp and weft directions. Nevertheless, it is difficult to separate these two parts. Moreover, these different matrix damages tend to join themselves and pass throughout the layers. Hence, in a first attempt, all matrix damages are to be gathered in a single element. Once more, this hypothesis limits the model to qualitative tool or numerical illustration of a proposed crack growth mechanism. This modelling choice gather different matrix regions, namely the resin surrounding the weft tows, the one surrounding the warp tows and the last one joining these two reinforcement directions [12,13]. Obviously, it is not possible to split the matrix in such way in reality which leads to putting alone the longitudinal fibres of the layer (Fig. 1).

The transverse fibres are then integrated into the matrix layer. These fibres are assumed to be unloaded when the matrix is fully cracked and thus bring no stiffness in the loading direction. Figure 1 illustrates the model, considering the warp yarns oriented in the loading direction. This description could also be applied to the weft direction of the fabric. The two layers are then linked together owing to user spring elements which characterise both the behaviours of the warp/weft interface and the resin contained in the warp and weft tows. In the limit case of a fully damaged matrix, these elements have a null stiffness; the strength is only due to the layer of fibres parallel to the loading direction.

The 2D-generalization of the previous sketch produces a symmetric model described below (Fig. 2). The behaviour of a woven ply can be seen as two superimposed meshes linked by spring elements with adjustable stiffness. Each mesh corresponds to either

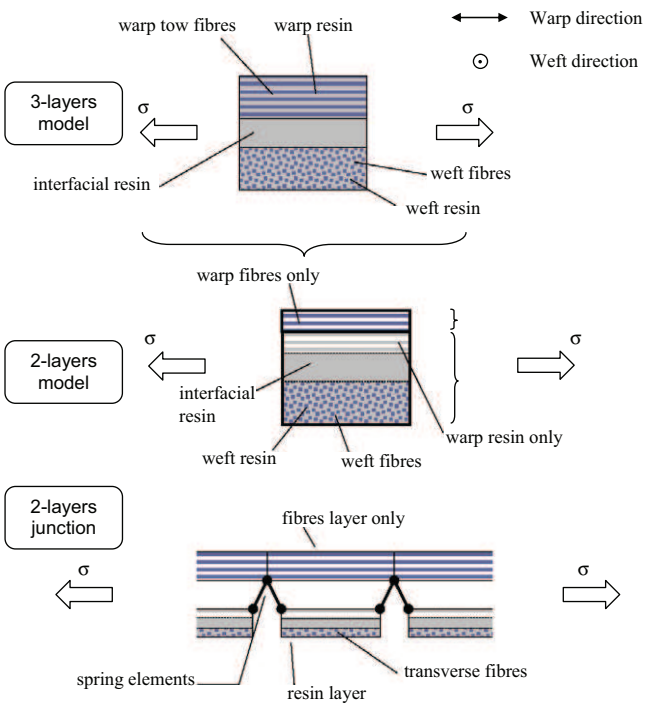

Fig. 1. 1D modelling approach for a woven ply.

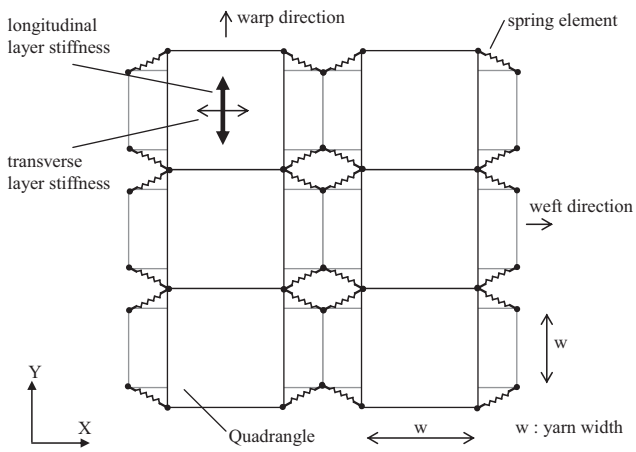

Fig. 2. Finite element model for a woven ply.

the warp or the weft reinforcement direction. The meshes are built with the same level of refinement: each quadrangle is a 0.5 mm sized square which is equal to the yarn width. The two superimposed meshes of the same size have been deliberately distorted in order to reveal easily the linking spring elements.

These spring elements have initially a null length. Each fibre tow is modelled by a number of linear orthotropic plane stress elements sharing consecutively a couple of nodes. The load transfer between warp and weft directions is thus due to spring elements. On the other hand, parallel fibre yarns are just linked together through these spring elements.

The core of the model thus lies in managing the stiffness evolution of link elements which split up more or less:

- The two superimposed meshes which model the reinforced directions of the woven ply.
- The successive fibre yarns in the same direction.

3. Model identification

The elastic coefficients of the model are identified with the help of static and fatigue tensile tests [9]. In both cases, the maximum damage is near 30%. The fibres layer is then assumed to contribute to 70% of the initial stiffness of the woven ply, whereas the complementary part is brought by the matrix layer. The shear modulus and Poisson's coefficient of the woven ply are used as the remaining elastic coefficients of the plane stress elements.

3.1. Warp and weft direction in static

The studied woven ply is balanced, but exhibits different behaviours in warp or weft directions when loaded, mainly in the non-linear part of the stress–strain curve [9]. The behaviour law of user elements linking the warp and weft layers has to be defined. For tensile test in warp direction, the flexibility δ of spring elements is assumed to follow a linear relation with the warp fibre strain $\varepsilon(t)$ given by plane stress elements:

$$\delta = \frac{\varepsilon(t) - \varepsilon_c}{\eta_c} \tag{1}$$

where ε_c is the damage threshold value of the longitudinal strain and η_c is a damage coefficient in warp direction. From the monotonic tensile curves in warp and weft directions (Fig. 3), the coefficients values are identified (Table 1). The threshold value ε_c corresponds to the "knee-point" strain [14].

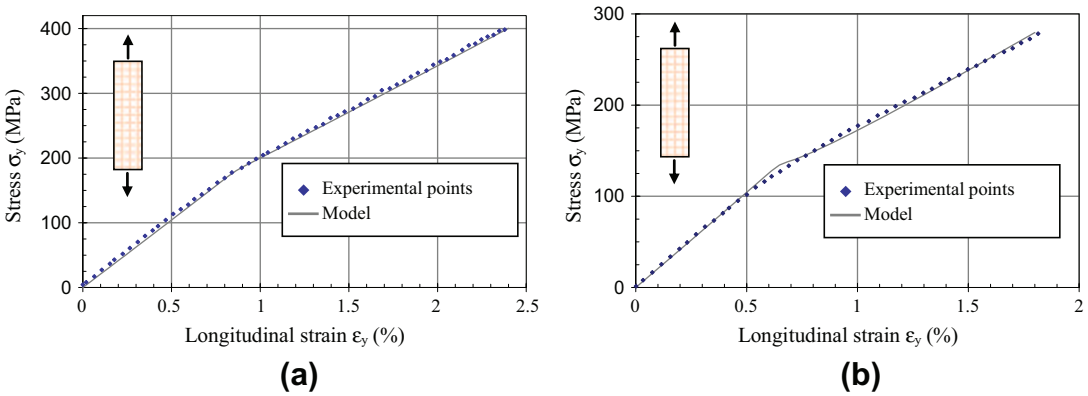

Fig. 3. Identification of the model coefficients in static tensile test for warp (a) and weft (b) directions.

Table 1
Stiffness parameters values of link elements.

Static behaviour	Threshold strain value (ε_c)	Damage coeff. η_c (N mm^{-1})
Warp	8.0×10^{-3}	40
Weft	6.0×10^{-3}	15
Static behaviour	Threshold distortion (γ_{lt}^0)	Damage coeff. η_s (N mm^{-1})
±45	1.0×10^{-2}	2.0
Fatigue at $\varepsilon_{max} = 3 \times 10^{-3}$	Asymptotic stiffness k_1 (N mm^{-1})	Curvature parameter α
Warp	13,000	1500
Weft	3000	1500

The same approach is undertaken for weft direction. The matrix damage occurs earlier and is more pronounced. This could be explained because the weft tows present a more severe crimp and are not necessarily aligned with each other unlike warp ones.

3.2. $[45]_2$ static behaviour

In a similar way, the flexibility δ of spring elements can be deduced owing to the static tensile tests on $[45]_2$ laminates (Fig. 4) and is chosen in a first attempt to be function of the angular distortion $\gamma_{lt}(t)$ given by 2D-elements:

$$\delta = \frac{\gamma_{lt}(\mathrm{t}) - \gamma_{lt}^0}{\eta_s} \tag{2}$$

where γ_{lt}^0 is the distortion corresponding to the beginning of degradation and η_s is the related damage coefficient (Table 1).

The finite element prediction of the deformed shape is in good agreement with the experimental one (Fig. 5). Examination of the fractured section indicates that the fibres are not broken completely, and on the other hand a huge sliding parallel to fibres direction appears breaking the loading path. Just one 2D-mesh is printed on the figure in order to make the comparison easier. The very small stiffness of some link elements creates sliding strips which are alike the experimental ones. However, the model does not take into account the inelastic strains that occur in such laminates. The model will be modified and improved in future to incorporate this anomaly.

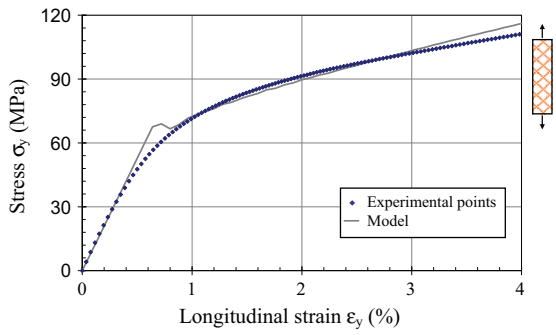

Fig. 4. Identification of the model coefficients in static tensile test for $[45]_2$ laminate.

3.3. Fatigue modulus decay of warp and weft laminates

The experimental results of fatigue crack growth in warp and weft laminates showed that the initiation duration played a key role in the maximum reached crack growth rate [9]. The more the initiation duration lasts, the less the crack growth rate level is important. This observation can be explained by the smoothing of stress concentration in notch tip due to matrix damage which even provokes the slowing down of crack growth. As the warp direction presented a lesser decrease of fatigue modulus than in the weft one, the initiation duration is overall lower in this direction. Given the influence of initiation duration on the crack growth, namely the diffuse microcracks in fatigue during this period, it seems useful to consider this phenomenon in the model.

Depending on the specimen width, the initiation duration corresponds to at least 50% of the fatigue crack growth tests duration. During fatigue tests on unnotched specimens led in strain control environment at maximum strain $\varepsilon_{max} = 3 \times 10^{-3}$ and ratio $R = \varepsilon_{min}/\varepsilon_{max} = 1/3$, a loss of modulus has been recorded in warp and weft directions [9]. In order to take into account this degradation, the flexibility δ of spring elements is chosen to vary with the number of cycles N in millions, with the asymptotic value of spring stiffness k_1 and with a curvature parameter α (Eq. (3)). The factor

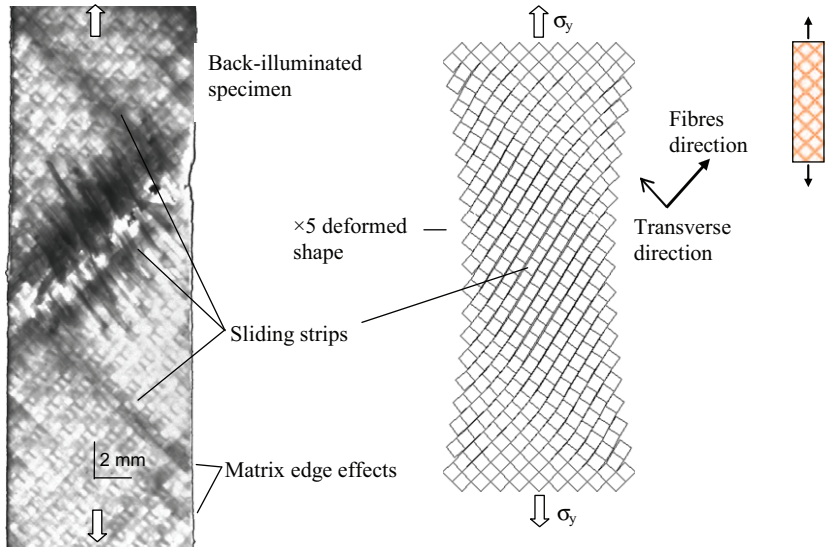

Fig. 5. Predicted and experimental deformed shape for $[45]_2$ laminate in static tensile configuration.

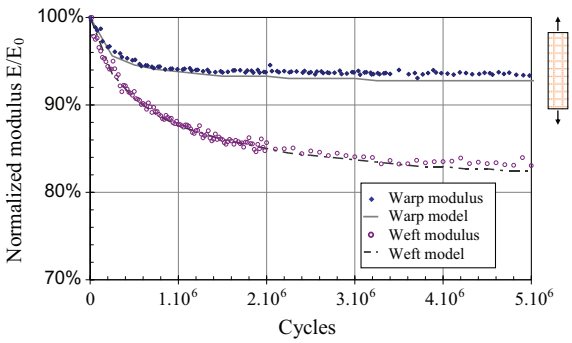

Fig. 6. Modulus decay in fatigue of the warp/weft direction of the studied glass woven ply at a maximum strain $\varepsilon_{max} = 3 \times 10^{-3}$.

k_0 corresponds to the initial value of stiffness of spring elements which is theoretically infinite (Fig. 6).

$$\delta = \frac{1}{k_1 + (k_0 - k_1).\frac{\log(1+\alpha \cdot N)}{\alpha \cdot N}} \tag{3}$$

The coefficients are identified for both warp and weft directions (Table 1). The coefficients k_1 and α should be a function of the fatigue maximum strain of fibres ε_{max}. However, with only a few experimental results in fatigue to other maximum strain levels, it seems difficult to identify the relation of these coefficients k_1 and α with the fatigue maximum strain. But, several experimental results from [15–17] on unnotched woven glass laminates tested in fatigue at load control give room for some assumptions.

The fatigue modulus decay is important in the first fatigue cycles such as $N/N_f < 20\%$, where N_f is the number of cycles to failure. This first stage is usually referred to phase *I*. The modulus decay is more important and quicker if the maximum stress in fatigue exceeds the "knee-point" stress. Echtermeyer et al. [16] underlined that the asymptotic ratio of the fatigue modulus over the static one $E_f(N)/E_0$ is equal to 70%. Consequently, the failure occurs between 10^3 and 10^4 cycles when the maximum fatigue stress exceeds the one associated with the "knee-point". Hence, the degradation in fatigue of the links between warp and weft directions is even faster since the maximum strain in fatigue has surpassed the "knee-point" strain. So, for strain levels greater than the "knee-point" one, the flexibility of spring elements is assumed to vary with a very high coefficient α. Their stiffness reaches therefore in few cycles the asymptotic stiffness k_1. In a simple way, the relationship between this value of asymptotic stiffness k_1 and the maximum fatigue strain just needs to be identified.

This relationship is evaluated thanks to the two following remarks:

- The fatigue tensile tests on $[0/90]_n$ at a maximum strain level of $\varepsilon_{max} = 6 \times 10^{-3}$ demonstrates that the asymptotic value of spring stiffness is reached at almost 5×10^5 cycles [9]. The measured crack growth rates in $[0]_2$ laminates are between 10^{-4} and 10^{-3} mm/cycle. Considering that the degradation of spring stiffness begins for a strain of $\varepsilon = 6 \times 10^{-3}$ without totally uncoupling the two layers is thus a reasonable approximation.
- The warp/weft links are assumed to be entirely damaged just before the fatigue failure of the fibres. With the help of previous experimental results, the fatigue lifetime of woven glass laminates loaded in the fibres direction is around 10^3 cycles when the ratio of the maximum fatigue stress over the ultimate tensile stress is equal to $\sigma_{max}/\sigma_{UTS} = 60\%$. This level corresponds to a strain of $\varepsilon_{fibres} = 1.2 \times 10^{-2}$ for the studied material.

Finally, the relationship between the spring stiffness and the maximum strain in fatigue is assumed to be linear in a logarithm scale between the two previous identified points:

$$k = k_0 \exp^{-\beta \cdot \langle \varepsilon_M - \varepsilon_{knee\text{-}point} \rangle_+} \tag{4}$$

where $k_0 = 10^6$ N mm^{-1} is the initial value of stiffness, $\beta = 2300$, $\varepsilon_{knee\text{-}point} = 6 \times 10^{-3}$ the "knee-point" strain, and $\langle x \rangle_+$ corresponds to the positive part of x (Fig. 7). The stiffness degradation begins for a fibres strain equal to the "knee-point" longitudinal strain. The coefficient β is identified in considering that the warp/weft links are nearly broken after few fatigue cycles.

3.4. Unified matrix damage law

The observed damage consists primarily of matrix cracks localized to the cross-over points of the fabric. Whatever the type of test, the damage has been modelled by the degradation of the stiffness of warp/weft link elements. The previously identified flexibilities are to be added. This modelling is close to the works of [6]

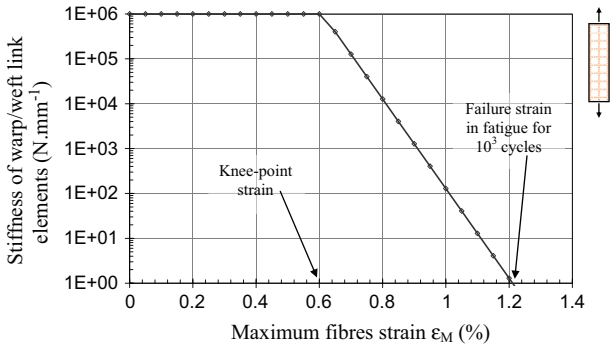

Fig. 7. Fatigue stiffness degradation of links elements vs. maximum fatigue strain of fibres.

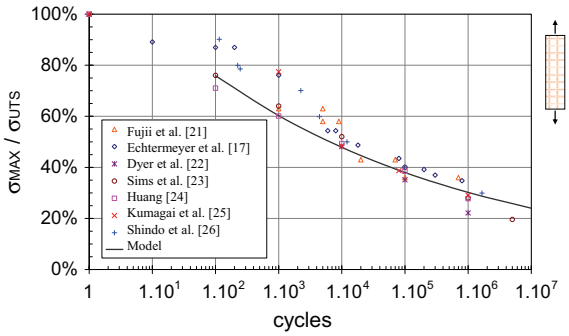

Fig. 8. Fatigue failure in tension of $[0]_n$ glass woven laminates.

which chose to sum the damage in static and those in fatigue of fabric based laminates.

An exponent n_0 is introduced in order to avoid drowning the low damage, especially that due to fatigue loads at a maximum strain level of $\varepsilon_{max} = 3 \times 10^{-3}$. Then the influence of crack initiation duration is made possible on the crack growth rate in warp and weft laminates of width 30 mm. The damage law of the warp/weft link elements can be summarised through the following equation:

$$\delta = \left(\delta_1^{\frac{1}{n_0}} + \delta_2^{\frac{1}{n_0}} + \delta_3^{\frac{1}{n_0}} + \delta_4^{\frac{1}{n_0}}\right)^{n_0} \tag{5}$$

where δ is the flexibility of link elements, n_0 is the weight coefficient, δ_1 is the flexibility identified on the static tensile tests in the unnotched laminates $[0]_2$ and $[90]_2$ given by Eq. (1), δ_2 is the flexibility identified on the static tensile tests in the unnotched laminates $[45]_2$ rendered in Eq. (2), δ_3 is the flexibility identified on the fatigue tensile tests at low strain level in unnotched laminates $[0]_2$ and $[90]_2$ expressed in Eq. (3) and δ_4 is the flexibility defined by tensile fatigue tests at strain levels above the "knee-point" in the unnotched laminates $[0]_2$ (Eq. (4)).

From the number of initiation cycles found for each specimen [7] and the modelling results, the value of exponent n_0 is set to $n_0 = 8$. This value is high because the fatigue damage associated with low strain level given by δ_3 just modifies a little the total flexibility δ of spring elements. The influence of δ_3 is therefore increased on the flexibility δ. The shapes and magnitudes of simulated curves with a value of $n_0 = 8$ are in agreement with the experimental ones. As a first approximation, a single coefficient n_0 is introduced but further studies are needed to clarify this sum of damage. Actually, this coefficient n_0 limits the realistic physical meaning of this model and should be, in the future, be evaluated thanks to simpler and different experimental tests of the crack growth.

3.5. Fibres fatigue failure law

In order to predict the crack growth, the fatigue strength of fibres in woven fabrics is used while assuming that a tow breaks entirely [18,19]. As the microscopic investigations showed [7], the crack remains stationary in a given position for a number of cycles of stress until a tow fails, where upon the crack extends by one tow width. The longitudinal stress value in tow thus allows to evaluate its lifetime. Moreover, as the tow width is constant and equal to 0.5 mm, the crack growth rate is calculated. The crack growth is associated with the fatigue behaviour of the glass fibres in woven fabrics. S–N curves of unnotched woven glass laminates are chosen to assess the lifetime of each tow. The experimental results of several authors [16,20–25] are considered to identify this fatigue behaviour law (Fig. 8). A Basquin-type law (Eq. (6)) describes the fatigue strength of $[0]_n$ glass woven laminates which is valid between 10^3 and 10^6 cycles:

$$\sigma_{max} = \frac{A_6}{N^{\gamma}} \tag{6}$$

where σ_{max} is the maximum fibres stress in fatigue, A_6 the fatigue failure stress at 10^6 cycles, N the number of cycles to failure in millions and γ, a material parameter.

In this case, $A_6 = 108$ MPa and $\gamma = 0.1$. No significant difference is underlined between warp and weft direction may be because the tests are led in stress control and the number of layers varies between 4 and 16.

This approach is important, since it assumes that the crack growth is not governed by a LEFM phenomenon but by fatigue fracture of the tow in the crack tip. This hypothesis is supported by experimental observations showing a significant decoupling between the warp and weft tows in the crack tip [7]. The woven ply thus cannot be modelled using a single shell finite element in the thickness but two elements are needed with a coupling between them.

4. Numerical results and discussions

4.1. Warp $[0]_2$ and $[90]_2$ laminates

In the same way as the experimental campaigns, the predicted crack growths are studied on specimens of 30 mm and 50 mm widths with warp or weft direction aligned with the load:

- Specimen has a width of 30 mm with a UD carbon strip of 10 mm width and a notch length of 3 mm. This type of specimen has highlighted the importance of crack initiation duration on the level of crack growth rate and the different behaviours in propagation of warp and weft directions of the fabric studied [9].
- Specimen has a width of 50 mm with a UD carbon strip of 10 mm width and a notch length of 7 mm. This geometry allowed a quick initiation of crack [7].

The simulated results in samples of 30 mm width underline that the mean crack growth rate level is in good agreement with the experimental one. However, the corresponding crack length for maximum crack growth rate is not correctly predicted especially for specimens with high initiation duration (Fig. 9).

In this case, the longitudinal strain in the crack tip is constant whenever the crack length is between 5 and 15 mm. Obviously, the maximum crack growth rate position is well approximated for null initiation duration. The predicted crack growth rates exhibit unsteady evolution for crack initiation duration equal to zero. For others specimens, the fatigue induced damage seems to soften

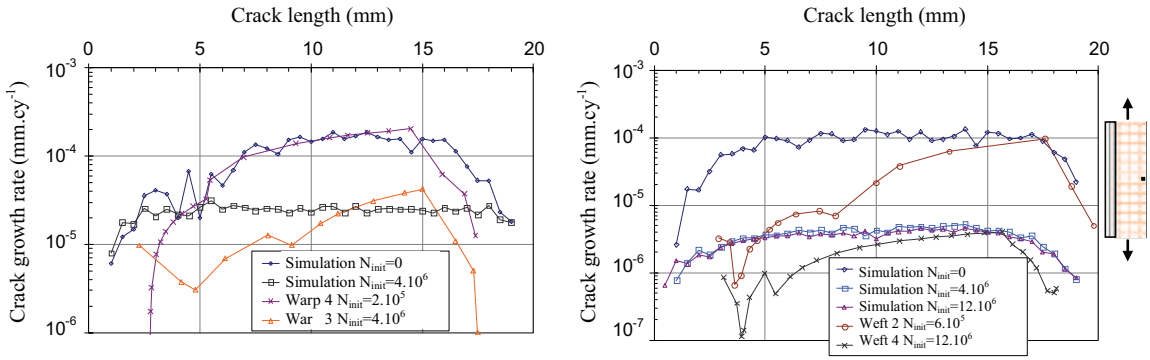

Fig. 9. Simulated crack growth rates in warp (a) and weft (b) laminates of 30 mm width.

the crack growth rate evolution. One way to improve this jagged evolution of simulated crack growth rate consists perhaps in mesh refinement respecting the tow geometric characteristics. Further developments are expected in future.

The initiation phase or stage I of crack growth is not well rendered by the model. This stage is ending when the crack growth rates reaches its minimum value i.e., the notch undergoes blunting. This lower value of crack growth rate can be associated to the development of a critical damage density which corresponds to the onset of stable crack growth acceleration.

The predicted crack growth rates in specimens of 50 mm width are consistent with the previous remark (Fig. 10).

As the notch length measures 7 mm, the experimental rates begin at that corresponding value whereas the simulated ones start for a crack length of 1 mm. The model expects maximum rates near 2×10^{-4} mm cy^{-1} while measured ones are between 3×10^{-4} and 5×10^{-4} mm cy^{-1} in warp laminates. Furthermore, the model does not present acceleration of crack growth, but expects constant rate for crack lengths between 10 and 30 mm. The model neglects cumulative damage effects for ligaments ahead of the crack tip because of the high stress gradients in the crack tip region. They should be taken into account to improve the crack growth rate prediction.

The model lacks accuracy, however, as a comprehensive model, it gets an insight into the damage phenomena in front and around the crack tip and especially on the relative sliding between warp and weft yarns. For instance, the strain field in loading direction ε_y reveals a good agreement with observed damage (Fig. 11).

In order to illustrate the comparison, the photographs of a crack are reproduced both on warp and weft faces of the fabric. The maximum value of the longitudinal strain in the crack tip yarn is $\varepsilon_y = 9.3 \times 10^{-3}$. In this yarn, the strain is overall constant for a height of 1.5 mm (Fig. 11a). The cross-over points of the woven plies are ideal places for fibre tow failure and it can be seen from the photographs (Fig. 11c) that the local crack path varies for a 1.5 mm height. It is also worth noting that the yarn in crack tip is disconnected from adjacent ones because the stiffness of spring elements providing the connection being very low. This scenario seems to agree with the experimental photographs (Fig. 11c) where matrix damage appears in the interstices of adjacent yarns.

The longitudinal strain field ε_y in transverse yarns can characterise the matrix damage (Fig. 11b). Due to the amplified deformed shape, the spring elements uncouple strongly the two superimposed meshes on 5 mm height which is consistent with experimental observations (Fig. 11d). Moreover, the matrix damage, modelled by the stiffness degradation of spring elements, is ahead of the crack tip by a distance of 1–1.5 mm (Fig. 11b) which is also consistent with experimental observations (Fig. 11d).

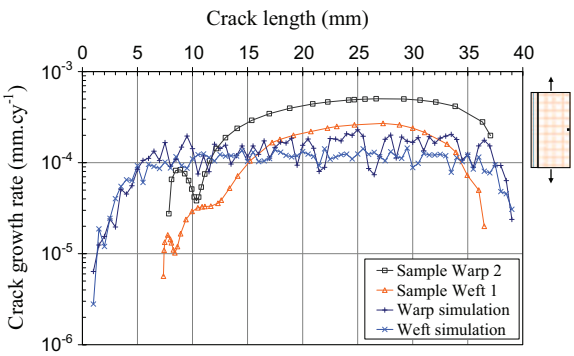

Fig. 10. Simulated crack growth rates in warp and weft laminates of 50 mm width.

4.2. $[45]_2$ laminates

The simulated crack growth rate is close to the experimental ones (Fig. 12).

The values given by the FE model evolve again in a jagged manner. The influence of the notch edge strip is correctly described but the simulated crack growth rate is higher than the experimental ones in the beginning of crack growth. For crack lengths between 10 and 20 mm, the model is in good agreement with the measured crack growth rates. The slowing down of crack growth for crack lengths greater than 10 mm is not predicted. This might be due to a damage phenomenon in fatigue but for the current study is not taken into account.

The analysis of the predicted strain field seems to confirm the appropriate choice of the model. To illustrate, figure 13 describes the strain field in the fibres direction near the crack tip. It should be point out that the model consists of two superimposed meshes. Just one mesh corresponding to the +45° fibres is visualized. The maximum strain in the fibres is in the crack tip direction which leads to the tow failure. The variable local direction of the crack is correctly predicted. As the deformed amplification is equal to 10, it is also possible to remark that the tow in the crack tip is disconnected with the neighbouring tows all along a length of 2 mm. This result is close to the microscopic investigations of longitudinal thin strips of damage between consecutives tows [7].

The model provides an important fibre strain gradient in the crack tip yarn. Yet, the model assumes that a yarn breaks entirely. So, in order to determine the lifetime of the yarn according to Eq. (6), the maximum strain value is retained. This is a clue which explains jagged rate curve and identifies rough mesh size. As expected, damage occurs in thin strips parallel to fibres direction. Finally, the analysis of damage around the crack is led to evaluate the relevance of the model (Fig. 14).

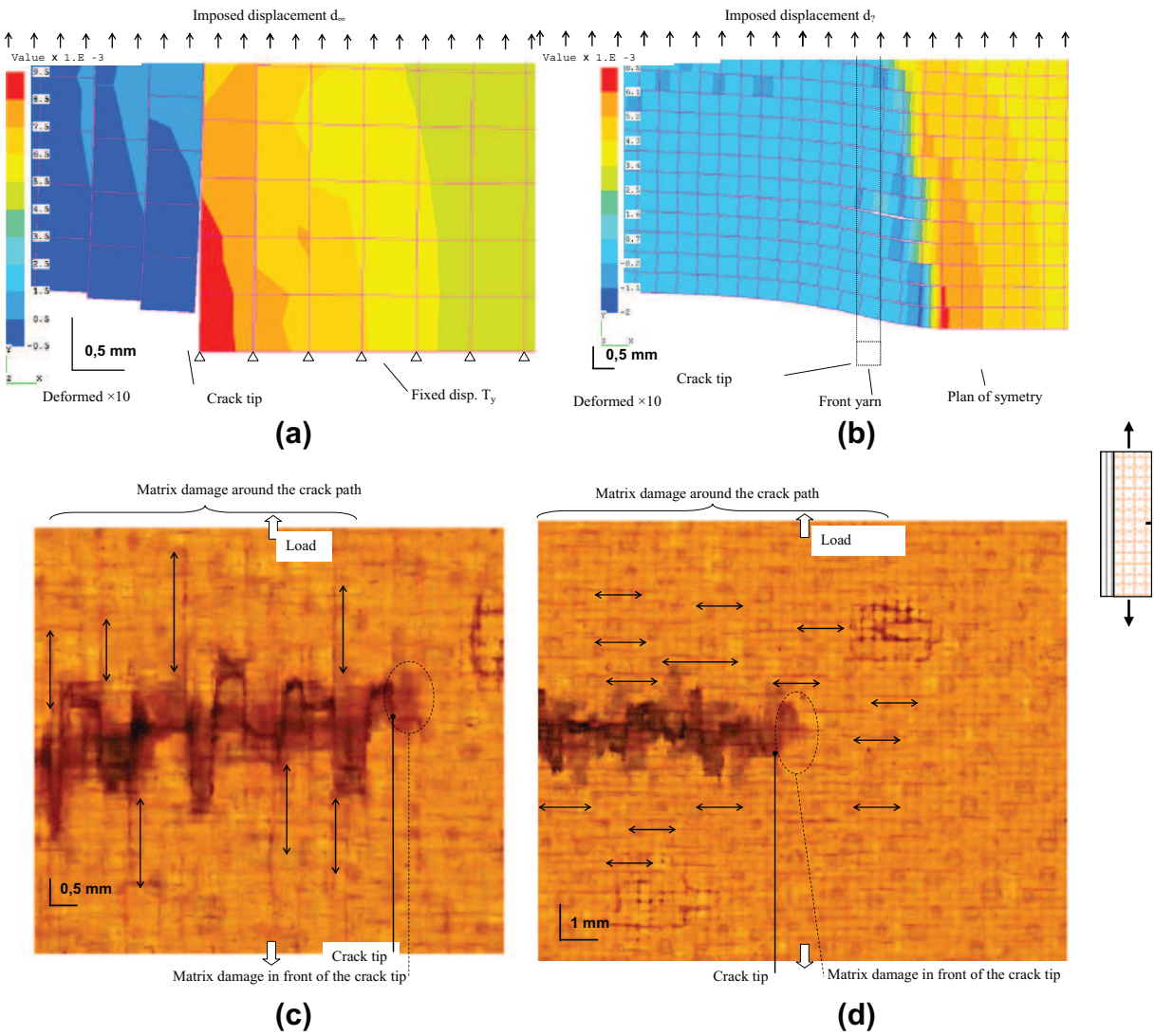

Fig. 11. Analysis of the strain field ε_y in yarns parallel (a) and perpendicular (b) to the loading direction and of the visible damage around the crack tip on warp (c) and weft faces (d).

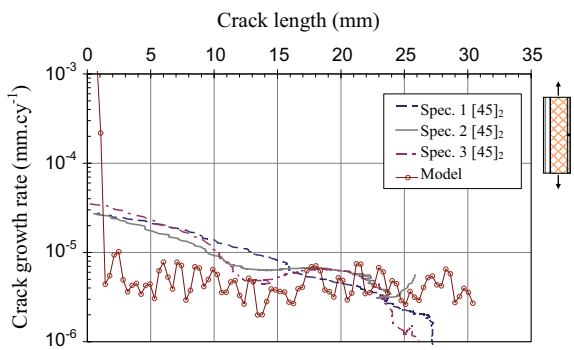

Fig. 12. Simulated crack growth rates in bias laminates of 50 mm width.

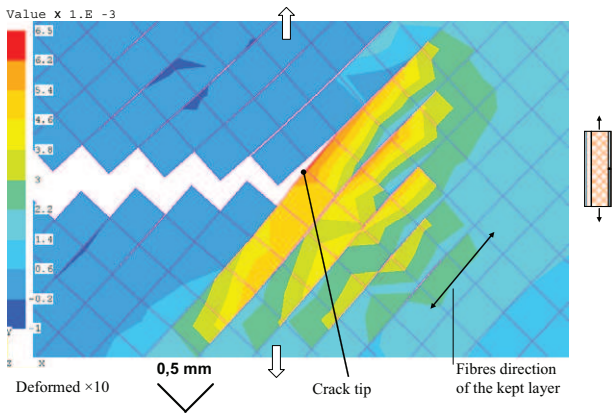

Fig. 13. Fibres strain field in the crack tip in $[45]_2$ laminates.

The initial stiffness of spring elements is equal to 10^6 N mm^{-1} which is theoretically infinite and corresponds to a perfect bond between the two layers of the model. The stiffness then decreases with the increasing matrix damage. The loss of stiffness is very important near the notch tip because of the carbon strip on notch edge of the specimen acting as a trailing edge where the initial value can be divided by a factor of 10^5 minimum. With the increasing crack length, the damage tends to be smaller. Furthermore, a slight asymmetry of degradation between the two directions exists which might be due to the fact that the chosen mesh size is not

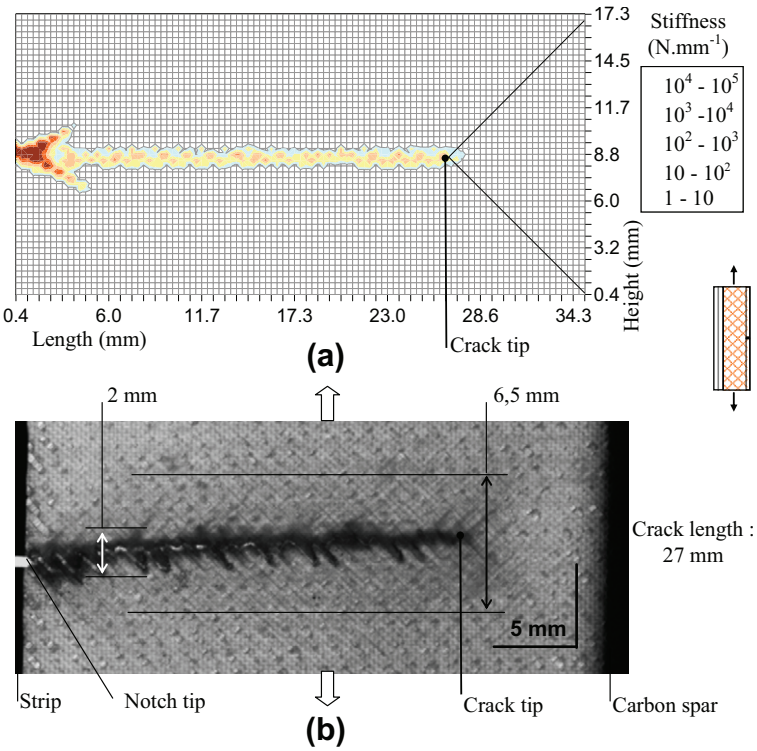

Fig. 14. Analysis of the simulated (a) and the visible damage (b) in $[45]_2$ laminates.

appropriate. The average value of the degraded stiffness is between 10^3 and 10^4 N mm^{-1} and damage exists ahead of the crack tip. In addition, damage goes with the crack on a relatively constant height of about 1.5 mm.

Long and thin strips associated with matrix damage between two neighbouring yarns are observed around the crack up to 6.5 mm, which is far from that predicted by the model. But if matrix damage intensity is a good level indicator, then a strong damage of 2 mm height takes place around the crack which is consistent with model damage. A better understanding of fatigue damage in bias laminates, especially in terms of inelastic strain should improve the predicted results.

5. Conclusions

An original model has been developed to enhance the understanding of fatigue propagation of a through-the-thickness crack in woven glass laminates. The proposed FE model follows the own natural discretization of the fabric. The main damage that occurs in the woven ply also served as a guide for the model assumptions. It consists of meta-delaminations which progressively disconnect the two reinforcement directions. The localized damage was preferred over a diffused damage. The proposed model relies on the separation of fatigue behaviour of each component; i.e. matrix damage and fibres failure; of the studied composite material through the use of two superimposed meshes connected by specific damageable elements. Nevertheless, the pure behaviours of resin and fibres are not used to calibrate this model and limits its physical meaning. In fact, the objective of this model is to illustrate and to confirm a proposed crack growth mechanism. The comparison of model predictions with experimental results seems to confirm the correct orientation of the model. The model rates are in good agreement with the experimental ones. The matrix damage around and in front of the crack tip is well described in different laminates. This model gives an insight in the understanding of the phenomena involved in fatigue crack growth in woven laminates. It could bring additional information for more conventional models based on CDM.

References

[1] Marissen R, Westphal T, Sterk J. Fracture of quasi-isotropic composite sheets with sharp notches. Compos Sci Technol 2006;66:1803–12.
[2] Shindo Y, Inamoto A, Narita F. Characterization of mode I fatigue crack growth in GFRP woven laminates at low temperatures. Acta Mater 2005;53:1389–96.
[3] Poe C, Reeder J. Fracture behavior of a stitched warp-knit carbon fabric composite – Nasa/TM-2001-210868.
[4] Kennedy T, Cho M, Kassner M. Predicting failure of composite structures containing cracks. Composites Part A 2002;33:583–8.
[5] Coats T, Harris C. A progressive damage methodology for residual strength predictions of notched composite panels – Nasa/TM-1998-207646.
[6] Hochard C, Payan J, Bordreuil C. A progressive first ply failure model for woven ply CFRP laminates under static and fatigue loads. Int J Fatigue 2006;28:1270–6.
[7] Bizeul M, Bouvet C, Barrau JJ, Cuenca R. Fatigue crack growth in thin notched woven glass composites under tensile loading. Part I: Experimental. Compos Sci Technol 2011;71:289–96.
[8] Bizeul M. Study of the fatigue crack growth in thin composite skins made of woven plies, PhD thesis, Université de Toulouse; 2009. <http://www.oatao.univ-toulouse.fr/2354/>.
[9] Bizeul M, Bouvet C, Barrau JJ, Cuenca R. Influence of woven ply degradation on fatigue crack growth in thin notched composites under tensile loading. Int J Fatigue 2010;32:60–5.
[10] Alif N, Carlsson LA. Failure mechanisms of woven carbon and glass composites. Compos Mater: Fatigue Fract 1997;6:471–93 [ASTM STP 1285].
[11] Pandita S, Huysmans G, Wevers M, Verpoest I. Tensile fatigue behaviour of glass plain-weave fabric composites in on- and off-axis directions. Composites Part A 2001;32:1533–9.
[12] Feng Z, Allen H, Moy S. Theoretical and experimental investigation of progressive failure of woven composite panels. J Compos Mater 1999;33:1030–47.
[13] Mc Laughlin P, Santhanam S. Simulating damage growth in a [90/0]s composite laminate using quasi-two-dimensional finite element methods. Compos Struct 2002;58:227–36.
[14] Boniface L, Ogin S, Smith P. Damage development in woven glass fibre/epoxy laminates under tensile loading. In: 2nd International conference on

deformation and fracture of composites, proceedings, Manchester; 29–31 March 1993.
[15] Smith E, Pascoe K. Biaxial fatigue of a glass-fibre reinforced composite part 1: fatigue and fracture behaviour – biaxial and multiaxial fatigue, EGF 3. Mechanical Engineering Publications; 1989. p. 367–96.
[16] Echtermeyer A, Engh B, Buene L. Lifetime and Young's modulus changes of glass/phenolic and glass/polyester composites under fatigue. Composites 1995;26:10–6.
[17] Hansen U. Damage development in woven fabric composites during tension–tension fatigue. J Compos Mater 1999;33(7).
[18] Mandell JF. Fatigue crack propagation rates in woven and non woven fiber glass laminates. Compos Reliab ASTM STP 1975;580:515–27.
[19] Schulte K, Reese E, Chou T. Fatigue behaviour and damage development in woven fabric and hybrid fabric composites. In: Proceedings of the sixth international conference on composite materials (ICCM-VI), vol. 4. London; 20–24 July 1987.
[20] Fujii T, Amijima S. Microscopic fatigue processes in a plain-weave glass-fibre composite. Compos Sci Technol 1993;49:327–33.
[21] Dyer K, Isaac D. Fatigue behaviour of continuous glass fibre reinforced composites. Composites Part B 1998;29:725–33.
[22] Sims G, Broughton W. Comprehensive composite materials, vol. 2. Glass fiber reinforced plastics properties. p. 151–97, ISBN: 0-080437206.
[23] Huang Z. Micromechanical modeling of fatigue strength of unidirectional fibrous composites. Int J Fatigue 2002;24:659–70.
[24] Kumagai S, Shindo Y, Horiguchi K, Narita F. Tension–tension fatigue behavior of GFRP woven laminates at low temperatures. Mech Adv Mater Struct 2004;11:51–66.
[25] Shindo Y, Takano S, Horiguchi K, Sato T. Cryogenic fatigue behavior of plain weave glass/epoxy composite laminates under tension–tension cycling. Cryogenics 2006;46:794–8.